RESEARCH ARTICLE
doi: 10.2306/scienceasia1513-1874.2025.099

ScienceAsia 51 (6): 2025: ID 2025099: **1–9**

Preparation of a *Staphylococcus* phage endolysin and its antibacterial activity

Shihui Wang†, Yulu Wang†, Qiqi Cao, Zhenhong Yang, Qi Lin, Qiyun Guan, Xinger Lu, Bokun Lin*

School of Public Health, Shunde Women and Children's Hospital, Guangdong Medical University, Guangdong 528300 China

*Corresponding author, e-mail: bklin@gdmu.edu.cn
† These authors contributed equally to this work.

Received 23 Jul 2025, Accepted 4 Dec 2025
Available online 22 Dec 2025

ABSTRACT: A gene encoding a putative *Staphylococcus aureus* phage endolysin was identified in environmental virome samples. The gene was recombinantly expressed in *Escherichia coli* BL21 (DE3) using the pET-30a vector, and the resulting endolysin (designated as S2) was purified via affinity chromatography. Endolysin S2 demonstrated lytic activity against *S. aureus*. Furthermore, following pre-treatment with ethylenediaminetetraacetic acid (EDTA), endolysin S2 inhibited the growth of several Gram-negative bacteria, including *Salmonella enterica* serovar Enteritidis, *Salmonella enterica* serovar Typhi, *E. coli* and *Shigella*. Transmission electron microscopy revealed that treatment with endolysin S2 induced morphological distortions, cell wall damage, and a significant reduction in bacterial counts compared to the untreated control. Biochemical characterisation indicated that endolysin S2 had a pH optimum of 8.0 and retained over 95% of its relative activity within a broad pH range of 6.0 to 10.0. The optimal temperature for activity was 25 °C, with more than 90% relative activity retained at 37 °C.

KEYWORDS: bacteriophage endolysin, antibiotic resistance, viral metagenomics

INTRODUCTION

S. aureus, a Gram-positive bacterium [1], is a significant foodborne pathogen and a primary public health concern worldwide. The increasing prevalence of drug-resistant *S. aureus*, particularly methicillin-resistant *S. aureus* (MRSA) [2] and vancomycin-resistant *S. aureus* (VRSA) [3], poses a significant challenge to clinical management. Antibiotic resistance poses a significant threat to global public health. It is estimated that antimicrobial resistance could cause millions of premature deaths annually in the coming decades if it is not effectively contained [4]. Therefore, in addition to the rational and scientific use of existing antimicrobial drugs, the development of new complementary or alternative strategies is an urgent clinical need.

Bacteriophages are viruses that exclusively infect bacteria and are widely found in the environment, including the oceans, soil, and gut microbes of animals. They can be used as a non-antibiotic alternative for treating *S. aureus* [5]. However, their narrow host range often makes it challenging to identify a suitable phage for a specific bacterial pathogen. Furthermore, the preparation of phage therapeutics is technically demanding and requires rigorous purification to ensure the absence of bacterial toxins [6]. Endolysin, a peptidoglycan hydrolase, plays a crucial role in the terminal stage of the phage lytic cycle. Facilitated by holins, endolysins degrade the peptidoglycan layer of the bacterial cell wall, leading to lysis of the host cell and the subsequent release of progeny phages [7]. Compared to phages, endolysins are highly bactericidal and have a broader host spectrum, allowing for easy and targeted drug delivery, as well as low bacterial resistance [8].

Currently, the acquisition of phage endolysins relies on isolating and culturing phages from environmental samples, followed by genome sequencing and analysis to identify endolysin genes. Subsequently, the predicted endolysin genes are recombinantly expressed to produce the active endolysin. However, this culture-dependent approach is limited: approximately 99% of environmental viruses cannot be isolated using traditional culture methods [9]. Viral Metagenomics can completely bypass the limitations of conventional culture by directly extracting and sequencing viral nucleic acids from environmental samples (e.g., seawater, soil, the human microbiome). Capitalising on this advantage, we employed a viral metagenomics approach to identify and recover an endolysin gene from an *S. aureus* phage in environmental samples. Following gene cloning and recombinant expression, we successfully produced the endolysin, designated S2, which demonstrated potent antimicrobial activity.

MATERIALS AND METHODS

Strain sources

Bacterial strains of *S. aureus*, *Staphylococcus epidermidis*, and *Shigella* were obtained from Beina Biological Company (Beijing, China) and NovoPro Bio-Tech Ltd. (Shanghai, China). Additional strains, including *Salmonella* and *E. coli*, were obtained from the Centers

for Disease Control and Prevention of Shenzhzen city, China. All strains are maintained in our laboratory collection.

Environmental sample collection, viral particle enrichment, and nucleic acid extraction

River water samples were collected downstream of a large hospital and used as the environmental source in this study. A stainless-steel disc filter holder was connected to a peristaltic pump. The water sample was sequentially filtered through 1.6 μm and 0.22 μm glass microfiber membranes to remove large particulates and the most bacteria, allowing viruses to pass into the filtration. Subsequently, 1 M HCl was added to the filtrate to adjust the pH to 3.5. $FeCl_3$ was then added to a final concentration of 1 mg/l with thorough mixing. The mixture was incubated in the dark at room temperature for 2 h. This step facilitated the efficient enrichment of trace viruses by promoting viral aggregation via flocculation and co-precipitation with impurities. The mixture was then filtered through a 0.8 μm glass microfiber membrane. The membrane was removed, cut into thin strips, and transferred to a 50 ml centrifuge tube. Add 25 ml of virus resuspension buffer and incubate overnight at 4 °C in the dark to facilitate viral elution from the membrane. Following membrane discarding, we added NaCl (17.5 g/l) and PEG 8000 (8%) to the viral resuspension. The solution was homogenised completely and incubated overnight at 4 °C with constant agitation. This step uses high-salt conditions to remove the viral hydration layer, thereby reducing solubility and precipitating viruses from the larger-volume resuspension.

Following this, the solution was centrifuged at 12,000×g for 30 min. Discard the supernatant to obtain the viral pellet, then resuspend it in 1 ml phosphate-buffered saline (PBS) solution to achieve secondary concentration. To remove contaminating free nucleic acids, the resuspension was divided equally into four aliquots in 1.5 ml centrifuge tubes. DNase (10 μl) and RNase I (3 μl) were added to each tube, followed by incubation at 37 °C for 60 min. Subsequently, 7 μl of 0.1 M EDTA was added, and the mixture was incubated at 65 °C for 10 min to terminate enzymatic digestion and protect the released viral nucleic acids. Finally, viral nucleic acids were extracted using the QIAamp Viral RNA Mini Kit (Qiagen, Hilden, Germany) following the manufacturer's instructions.

Viral gene amplification, viromics sequencing, and phage endolysin gene analysis

First-strand cDNA was synthesised by reverse transcription using random primers harbouring a specific sequence tag. During second-strand synthesis, these tagged primers were incorporated at the 5′ ends of the cDNA. The double-stranded cDNA was subsequently amplified by PCR using complementary primers to the introduced sequence tag, enabling unbiased and highly efficient amplification of unknown sequences. The resulting viral nucleic acid amplicons were subjected to high-throughput sequencing by Magi Gene Biotechnology Ltd. (Guangdong, China) for viral metagenomics analysis. Functional annotation of the sequencing data was subsequently carried out to identify putative *S. aureus* phage endolysin genes.

Bioinformatics analysis of endolysin

Nucleotide sequences were translated into amino acid sequences with EMBOSS Transeq. The physicochemical properties of the resulting proteins were assessed with the ExPASy ProtParam tool. Protein homology was evaluated using NCBI's protein-protein BLASTp, and conserved structural domains were identified via MOTIF Search.

Synthesis of the endolysin gene and its recombinant plasmid construction and transformation

For molecular cloning, the target endolysin gene (obtained from viromics sequencing) was synthesised by NovoPro Bio-Tech (Shanghai, China) Ltd., with incorporated NdeI and XhoI sites at its termini. The pET-30a vector was selected for cloning and expression, as its T7 lac promoter facilitates high-level transcription of the target gene in *E. coli* BL21 (DE3) cells. The kanamycin resistance marker facilitates screening of recombinant plasmids, while the His-Tag, designed to flank the multiple cloning sites, enables rapid purification of recombinant endolysin via nickel-affinity chromatography. The synthesised endolysin gene and the pET-30a plasmid were both digested with NdeI and XhoI restriction enzymes for directional cloning. The resulting DNA fragments were separated by agarose gel electrophoresis, and the linearised vector and the target gene insert were purified from the gel. The target gene and pET-30a plasmid were ligated using T4 DNA ligase at 16 °C, resulting in the expression plasmid pET30a-S2. The ligation product was transformed into *E. coli* TOP10 competent cells. The transformants were selected on LB agar plates supplemented with 50 μg/ml kanamycin and incubated overnight at 37 °C. A single positive colony was selected from the transformation plate and inoculated into LB liquid medium containing kanamycin. The culture was incubated at 37 °C with shaking at 200 rpm for 8 h. The recombinant plasmid was extracted and verified by colony PCR and DNA sequencing to confirm the identity and integrity of the endolysin gene insert.

Expression, purification, and concentration of endolysin

The recombinant plasmid pET30a-S2 was transformed into *E. coli* BL21 (DE3) cells. Positive clones were selected and cultured, and protein expression was induced by adding 0.1 mM IPTG at 37 °C with shaking at 200 rpm for 4 h. Cells were harvested by

centrifugation, resuspended in buffer, and lysed by ultrasonication. Following centrifugation, the clarified supernatant was collected. Protein expression was assessed by 12% SDS-PAGE, and gels were visualised by Coomassie Brilliant Blue staining. Pick a single colony expressing the correct protein and inoculate it into LB liquid medium containing 50 μg/ml kanamycin. Incubate at 37 °C for 12 h, then transfer the culture at a 1:100 ratio to 100 ml of LB liquid medium. When the optical density (OD_{600}) reached 0.6–0.8, protein expression was induced by adding IPTG to a final concentration of 0.1 mM. Then, incubate the culture at 37 °C while shaking at 200 rpm for 4 h. These conditions were determined to be optimal for induction. Centrifuge at 10,000 rpm for 5 min and wash the cells twice by repeating this step. Resuspend the resulting pellet in Buffer A (50 mM Tris, 500 mM NaCl, pH 8.0). Next, sonicate the cells and centrifuge to collect the supernatant. Following the protocol of the protein purification kit (Beyotime Biotechnology, Shanghai, China), the nickel column was equilibrated twice before the supernatant was applied. Subsequently, the column was eluted stepwise: first with Buffer B–E (50 mM Tris, 500 mM NaCl, pH 8.0) containing 20–50 mM imidazole, and then five times with Buffer F–J (50 mM Tris, 500 mM NaCl, pH 8.0) containing 100–500 mM imidazole. A 20 μl aliquot from each elution fraction was collected for electrophoretic analysis.

The purified protein fractions were pooled and concentrated using a 10 kDa molecular weight cut-off (MWCO) ultrafiltration tube by centrifugation at 4,500×*g* and 4 °C. The concentrated protein was stored at 4 °C for subsequent experiments. Protein concentration was determined using the bicinchoninic acid (BCA) protein assay kit (Beyotime Biotechnology). Briefly, a standard curve was prepared using a protein standard according to the manufacturer's instructions. The absorbance was measured at 562 nm using a microplate spectrophotometer, and the sample protein concentrations were calculated.

Direct action of endolysin on *Staphylococci*

A frozen glycerol stock of the bacterial strain was retrieved from −80 °C storage, thawed, and inoculated into LB liquid medium at a 2% (v/v) inoculum. The culture was incubated at 37 °C with shaking for 12 h. The following day, the bacterial culture was streaked onto a solid LB agar plate to obtain single colonies. After incubation at 37 °C for approximately 12 h, a single colony was picked and inoculated into fresh LB liquid medium. This culture was incubated at 37 °C with shaking at 200 rpm until it reached the mid-log phase, yielding a fresh bacterial suspension. A 2 ml aliquot of the bacterial suspension was centrifuged at 8,000×*g* for 5 min. The pellet was washed and resuspended in PBS. This washing step was repeated twice, and the final cell suspension was adjusted to an OD_{600} of 0.8–1.0. Subsequently, 200 μl of the bacterial suspension (for various Staphylococcus species) was added to the wells of a 96-well microtiter plates, followed by 20 μl of endolysin S2; wells containing bacteria with PBS instead of endolysin served as the negative control. The plate was mixed gently and incubated at 37 °C for 2 h, after which the OD_{600} was measured. Experiments were performed in triplicate. The inhibition rate was calculated as follows: Inhibition rate (%) = [(OD_{600} of control group − OD_{600} of experimental group)/OD_{600} of control group] × 100%.

Effect of pH on endolysin activity

S. aureus ATCC 12600 cells were harvested, washed, and resuspended in 20 mM Tris-HCl buffers adjusted to different pH values (ranging from 3 to 12). Subsequently, 200 μl of the cell suspension was mixed with 20 μl of a 150 μg/ml endolysin S2 solution. The mixture was measured immediately at OD_{600} and again after incubation at 37 °C for 2 h. The assay was performed three times, and a control group was set up. Relative endolysin activity (%) was calculated as follows: Relative activity (%) = (OD_{600} decrease value/OD_{600} maximum decrease value for each group) × 100%.

Effect of temperature on endolysin activity

The OD_{600} was measured immediately after mixing 20 μl of 150 μg/ml endolysin S2 and 200 μl of the *S. aureus* ATCC 12600 suspension. Then, OD_{600} was measured after 2 h in environments at 25 °C, 37 °C, 45 °C, 50 °C, 55 °C, and 60 °C. A control group was included, and all assays were performed in triplicate. The assay was performed three times, and a control group was set up. The relative activity of endolysin (%) is: (OD_{600} decrease value/OD_{600} maximum decrease value for each group) × 100%.

Cleavage profile of endolysin S2

Fresh bacterial cultures of different *Salmonella* serotypes and *E. coli* genotypes were harvested by centrifugation, and the pellets were washed three times. The bacterial pellets were then resuspended in 50 mM Tris-HCl buffer (pH 8.0) containing 0.1% Triton X-100, and the suspensions were adjusted to an OD_{600} of 0.8–1.0. Following treatment with 100 mM EDTA for 5 min, the bacterial cells were washed with Tris-HCl buffer, collected by centrifugation at 10,000 rpm for 3 min, and finally resuspended in Tris-HCl buffer. In 96-well microtiter plates, 40 μl of endolysin S2 (150 μg/ml) was mixed with 180 μl of bacterial suspension from either EDTA-pretreated Gram-negative bacteria or non-pretreated Gram-positive bacteria. The plate was incubated at 37 °C for 2 h, after which the OD_{600} was measured to assess the lytic activity.

Transmission electron microscopy analysis

Bacterial cultures were harvested at the exponential phase to observe the effect of endolysin S2 on bacterial cell morphology using transmission electron microscopy (TEM). The bacterial cells were pre-treated with 1 mM EDTA at 37 °C for 5 min and then immediately centrifuged at 8,000 rpm for 2 min. The supernatant was discarded to remove EDTA, and the cell pellet was washed with PBS and adjusted to an OD_{600} of 1.0. Purified endolysin S2 (200 μg/ml) or buffer (control) was added to the EDTA-pretreated bacterial suspensions. Additionally, a bacterial suspension without EDTA pretreatment was included as another control. After incubation at 37 °C for 2 h, cells from the endolysin S2-treated and buffer-treated groups (both EDTA-pretreated), as well as *S. aureus* (which did not require EDTA pretreatment), were washed three times with PBS. The cells were then fixed with 2.5% glutaraldehyde for 3 h, followed by two gentle washes with PBS. The samples were stained with 1% phosphotungstic acid for approximately 1 min and observed with a Hitachi transmission electron microscope (Hitachi, Akishima-shi, Japan).

Statistical analysis

Excel was used to organise the data, and GraphPad Prism (version 8.0.2) was employed to analyse the data and plot the graphs. The results are presented as mean ± SEM ($n = 3$), and a one-way analysis of variance (ANOVA) followed by a multiple comparisons test was used to assess the differences between the samples (the level of significance was $p < 0.05$).

RESULTS

Endolysins identified by metagenomic technology

Using viral metagenomic sequencing, a total of 902 endolysin genes were identified in river water samples collected downstream of a major hospital. Among these, five endolysin genes were derived from *S. aureus* phages, representing 0.9% of the total, whereas the remaining sequences originated from phages infecting non-target bacterial hosts. Following a multi-step screening procedure, which included the removal of host-derived sequences and sequence comparison using BLASTp against the NCBI databases, a single phage endolysin predicted to target *S. aureus* was selected for further investigation and was designated endolysin S2.

Homology analysis of endolysin

Endolysin S2 has the highest amino acid sequence homology with *S. aureus* phage vB-SauM-JDYN endolysin (No. WFG33865.1) at 100%. However, the functional properties of proteins with high sequence similarity to endolysin S2 have not been experimentally characterised. Based on this sequence homology, we hypothesised that endolysin S2, likely derived from an *S. aureus* phage, possesses bactericidal activity against *S. aureus*.

Molecular characterisation of the endolysin

Endolysin S2 consists of 496 amino acids and has a predicted molecular weight of 54.98 kDa. The instability index, which predicts a proteins stability under *in vitro* conditions, classifies a protein as stable if its value is below 40 (Table 1). Endolysin S2 exhibited an instability index below 40, indicating that it is a stable protein. The grand average of hydropathy (GRAVY) value serves as an indicator of protein hydrophilicity; a negative value denotes a hydrophilic protein, whereas a positive value suggests a hydrophobic one. The negative GRAVY value calculated for endolysin S2 reflects its hydrophilic nature, a characteristic that may facilitate its expression in the soluble fraction of the supernatant.

Prediction of conserved structural domains of endolysin

Endolysin S2, derived from an *S. aureus* phage, contains a cysteine- and histidine-dependent amidohydrolase/peptidase domain (CHAP domain, PF05257) that is responsible for its primary peptidoglycan-cleaving activity. This CHAP domain exhibits affinity for Ca^{2+} and is frequently found in conjunction with other peptidoglycan-cleaving domains. The prevalence of such multifunctional hydrolases suggests that they may act cooperatively to degrade specific substrates within the bacterial cell wall [10]. The N-acetylmuramoyl-L-alanine amidase domain (PF01510) binds Zn^{2+} and cleaves the amide bond between N-acetylmuramic acid and L-alanine in the peptidoglycan chain [11]. Although this domain typically exhibits little to no cleavage activity when expressed in isolation, it acts synergistically with the CHAP domain, resulting in a "1+1>2" enhancement of lytic activity when the two domains are co-expressed [12]. The bacterial Src homology 3 (SH3) domain (PF08460) mediates protein binding and is predicted to facilitate specific recognition and attachment to the bacterial cell wall

Table 1 Physicochemical characterisation of endolysin S2.

Item	Gene size (bp)	No. of amino acids	Molecular mass (kDa)	Isoelectric point	Instability index	Aliphatic index	GRAVY
S2	1488	496	54.98	10.09	37.88	22.83	−0.598

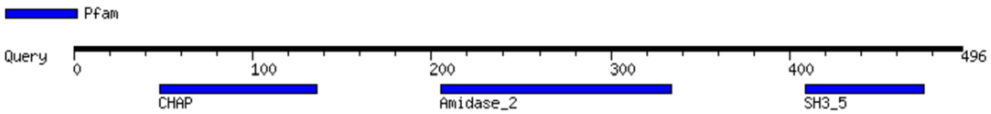

Fig. 1 Predicted conserved structural domains of endolysin S2.

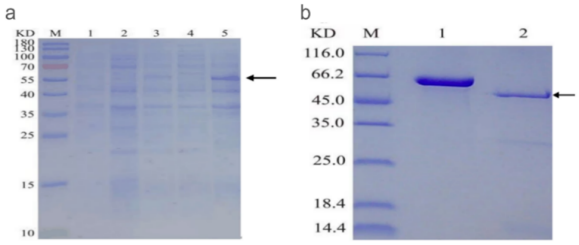

Fig. 2 SDS-PAGE analysis of recombinant endolysin S2 expression and purification. (a) SDS-PAGE of protein expression. M: protein ladders; 1: empty vector pET-30a control (induced); 2: *E. coli* BL21 (DE3) harbouring pET-30a-S2 uninduced; 3: *E. coli* BL21 (DE3) harbouring pET-30a-S2 induced; 4: pellet of induced cell lysate; 5: supernatant of induced cell lysate. The arrow points to the band corresponding to the target protein. (b) SDS-PAGE of purified protein. M: protein ladders; 1: protein standard; 2: purified endolysin S2. The arrow highlights the purified protein band.

[13]. A schematic representation of the domain architecture of endolysin S2 is provided in Fig. 1.

Expression and purification of endolysin

Based on a comprehensive review of both domestic and international literature on endolysin cloning and expression, as well as the characteristics of our target endolysin, the pET-30a vector was selected. The recombinant expression plasmid was constructed and verified by agarose gel electrophoresis and restriction enzyme digestion. The sizes of the resulting DNA fragments were consistent with those predicted by bioinformatics analysis. SDS-PAGE analysis of the supernatant of the recombinant bacterial lysate revealed a discrete band for endolysin S2 between 45 kDa and 66.2 kDa (Fig. 2a), indicating that the protein was successfully expressed in a soluble form. The soluble endolysin S2 was subsequently purified via a nickel-affinity column. The purity and identity of the purified protein were confirmed by SDS-PAGE (Fig. 2b). The final concentration of the purified endolysin S2 was determined to be 1500 μg/ml by BCA assay.

Endolysin alone acts on *Staphylococci*

The lytic activity of endolysin S2 against various *Staphylococcus* species was evaluated by monitoring turbidity reduction following incubation at 37 °C for 2 h. The results showed that endolysin S2 exhibited significant lytic activity against all ten tested

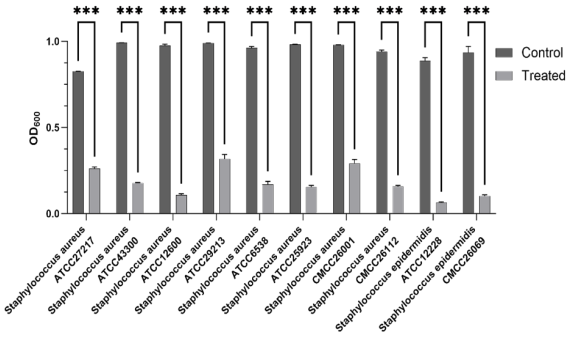

Fig. 3 Antibacterial activity of endolysin S2 against *Staphylococcus*. Data are presented as means ± SD ($n = 3$). Significant differences between groups are indicated by *, **, and ***, representing $p < 0.05$, $p < 0.01$, and $p < 0.001$, respectively.

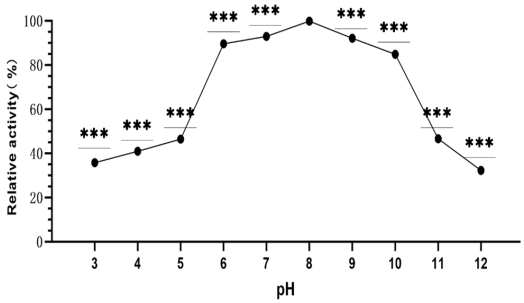

Fig. 4 Effect of pH on endolysin activity. Data are presented as means ± SD ($n = 3$). Significant differences compared to the group at pH 8.0 are indicated by *, **, and ***, representing $p < 0.05$, $p < 0.01$, and $p < 0.001$, respectively.

Staphylococcal strains, with inhibition rates exceeding 67%. Notably, the inhibitory effect was most pronounced against *S. epidermidis* ATCC 12228 and *S. aureus* ATCC 12600, with inhibition rates of 92.8% and 89.0%, respectively. These findings indicate that endolysin S2 exhibits broad-spectrum and potent anti-*Staphylococcal* activity (Fig. 3).

Effect of pH on endolysin activity

The effect of pH on the lytic activity of endolysin S2 against *S. aureus* is shown in Fig. 4. Endolysin activity was inhibited at pH values below 4 and above 10. When the pH ranged from 6 to 10, the endolysin exhibited high activity, with relative activity exceeding 85%. The optimal activity was observed at pH 8.

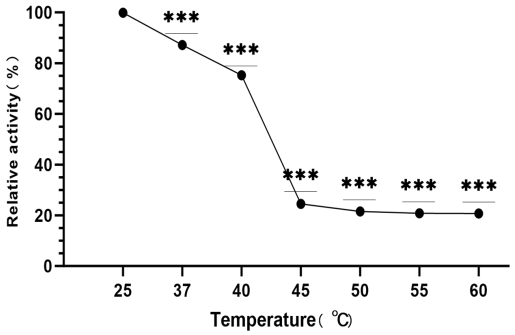

Fig. 5 Effect of temperature on endolysin activity. Data are presented as means ± SD ($n = 3$). Significant differences compared to the group exhibiting the highest relative activity are indicated by *, **, and ***, representing $p < 0.05$, $p < 0.01$, and $p < 0.001$, respectively.

Effect of temperature on endolysin activity

The effect of temperature on the activity of endolysin S2 is shown in Fig. 5. The optimal temperature for endolysin S2 activity was 25 °C. At 37 °C, the relative activity decreased slightly, remaining at approximately 90%. When the temperature exceeded 45 °C, the endolysin's relative activity sharply reduced to approximately 40%.

Cleavage profile of cleavage endolysin S2

The cleavage spectrum of endolysin S2 was examined via the turbidity reduction assay, and the results are presented in Table 2. Endolysin S2 exhibited lytic activity against eight different *S. aureus* strains, as well as against *S. epidermidis* CMCC26069, *Shigella sonnei*, and *E. coli* $escV^+$.

Transmission electron microscopy of endolysin-treated bacterial cells

To further visualise the lytic activity of endolysin S2, TEM was employed to observe morphological alterations in *Shigella sonnei* and *S. aureus* ATCC 12600. In the absence of treatment, the surfaces of bacterial cells was smooth and translucent (Fig. 6A,D and Fig. 7A,C); while in 100 mM EDTA pretreated *Shigella sonnei*, the bacterial surface was not ruptured, and it was in the form of spheres, rods, or bunches of grapes, and part of the bacterial outer membrane became loose and fuzzy (Fig. 6B,E). Compared with the control group, after 200 μg/ml endolysin S2 treatment for 2 h, the bacteria exhibited distorted morphology and damaged cell walls (Fig. 6C,F and Fig. 7B,D), and the number of bacteria was significantly lower than in the untreated group.

Table 2 Cleavage spectrum of endolysin S2 against various bacterial strains.

Host bacterial species	S2
Salmonella enterica serovar London [10:w:6]	−
Salmonella enterica serovar Typhimurium [4:i:2]	+
Salmonella enterica serovar Typhi [9)Vi:i:26]	+
Salmonella enterica serovar Weltevreden [10:r:Z6]	−
Salmonella enterica serovar Bovismorbificans [7:w:enx]	−
Salmonella enterica serovar Brænderup [7:oh:en215]	−
Salmonella enterica serovar Seahamurella [10:gs:t]	−
Salmonella enterica serovar Risperdal [68:w:lw]	−
Salmonella enterica serovar SaintPaul [4:en:2]	−
Salmonella enterica serovar Enteritidis	−
Salmonella enterica serovar Agona[4:fg:–]	+
Salmonella enterica serovar Infantis[7:r:5]	−
Salmonella enterica serovar Bulleiden[9:g:m:–]	−
Salmonella enterica serovar non-dinvolvulus[16:6:enx]	+
Salmonella enterica serovar Cotibus[68:eh:5]	−
Salmonella enterica serovar Giv[10:w:7]	−
Salmonella enterica serovar Kentucky[820:i:Z6]	−
Salmonella enterica serovar Stanley[4:d:2]	−
Escherichia coli $escV^+$, $astA^+$	+
Escherichia coli Lt^+, $astA^+$	−
Escherichia coli $aggR^+$, pic^+, $astA^+$	−
Escherichia coli Lt^+, sth^+, $astA^+$	−
Escherichia coli $escV^+$, pic^+	−
Escherichia coli sth^+, $astA^+$	−
Escherichia coli Lt^+	−
Escherichia coli pic^+, $astA^+$	−
Escherichia coli $aggR^+$, pic^+	−
Escherichia coli $escV^+$	+
Escherichia coli $astA^+$	−
Escherichia coli pic^+	−
Staphylococcus aureus ATCC27217	++
Staphylococcus aureus ATCC43300	++
Staphylococcus aureus ATCC12600	++
Staphylococcus aureus ATCC 29213	++
Staphylococcus aureus ATCC6538	++
Staphylococcus aureus ATCC 25923	++
Staphylococcus aureus CMCC26001	++
Staphylococcus aureus CMCC26112	++
Staphylococcus epidermidis ATCC12228	++
Staphylococcus epidermidis CMCC26069	++
Shigella sonnei	++
Shigella flexneri	+
Shigella dysenteriae	−
Plesiomonas shigelloides	−

Symbols in the table denote lytic activity: ++, substantial lysis (OD_{600} reduction > 70%); +, partial lysis (OD_{600} reduction 30%–70%); −, no lysis (OD_{600} reduction < 30%). Data are presented as mean ± SD from three independent experiments ($n = 3$).

DISCUSSION

The widespread use of antibiotics has led to the emergence of antimicrobial resistance (AMR), posing a serious threat to global public health. However, the development of new antibiotics lags well behind the evolution of drug-resistant bacteria. In particular, *S. aureus*, as a major pathogen posing a significant threat to human health [14], displays Multiple Drug Resistance (MDR) and Extensively Drug-Resistant (XDR) [15]. Therefore, the development of novel antimicrobial

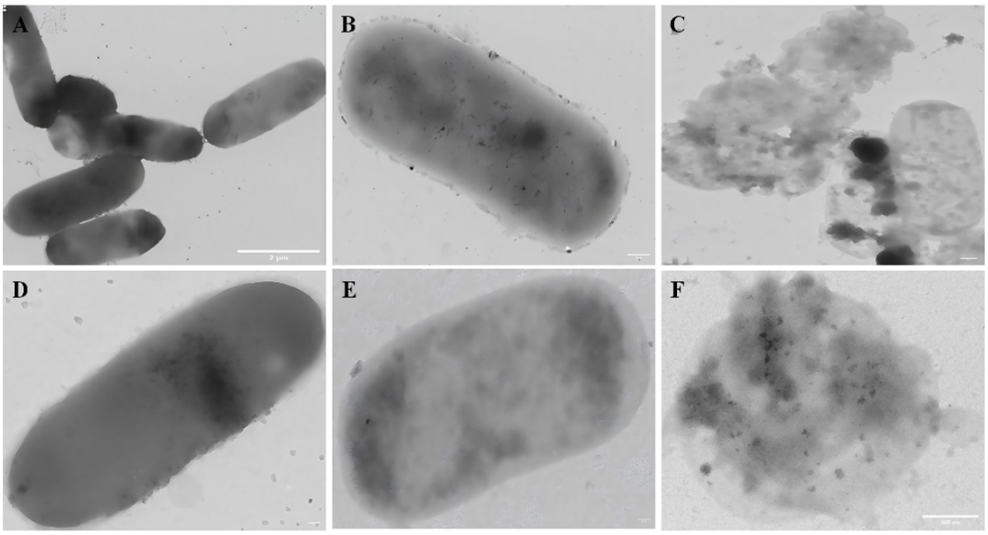

Fig. 6 Transmission electron micrographs of *Shigella sonnei* following treatment with endolysin S2. (A,D) PBS-washed cells; (B,E) EDTA-pretreated cells; (C,F) EDTA-pretreated cells incubated with 200 μg/ml endolysin S2. The scale bar corresponds to 2 μm (A–C) and 500 nm (D–F).

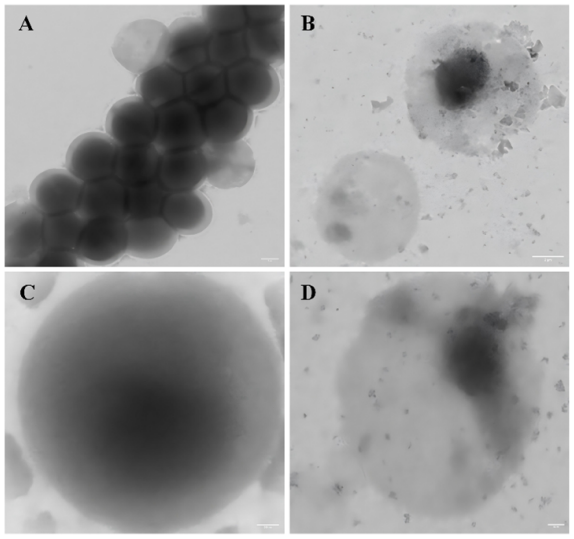

Fig. 7 Transmission electron micrographs of *S. aureus* ATCC 12600 cells following treatment with endolysin S2. (A,C) PBS-washed cells; (B,D) Cells treated with 200 μg/ml endolysin S2. The scale bar corresponds to 2 μm (A,B) and 500 nm (C,D).

agents is urgently required. Bacteriophages and their derived endolysins represent a promising class of alternatives to address this challenge. However, the use of live phages raises concerns regarding their long-term safety for *in vivo* applications. In contrast, endolysins, which are enzymes that degrade peptidoglycan, have a relatively simple protein structure and are considered safer for therapeutic use.

The conventional approach to obtaining phage endolysins involves isolating phages from culturable host bacteria, followed by genome sequencing, identification of endolysin genes, and recombinant expression of these genes. However, this method is significantly limited by the fact that approximately 99% of environmental microorganisms are uncultivable under laboratory conditions [9]. Consequently, the diversity of endolysins accessible through traditional phage isolation and cultivation is severely restricted. In contrast, metagenomics is a widely recognised technological approach capable of effectively obtaining sequence information for the entire environmental microbial community, including uncultivable microorganisms [16]. In this study, we collected river water samples near a large hospital and used viral metagenomics and high-throughput sequencing to identify novel bacteriophage endolysin genes. Through systematic bioinformatics analysis, including homology comparisons in databases such as NCBI, we identified and selected a putative endolysin, designated S2, predicted to possess lytic activity. Physicochemical analysis indicated that endolysin S2 exhibits high structural stability and maintains its activity *in vitro* for an extended period. Gene homology and conserved domain analysis confirmed that S2 belongs to the endolysin superfamily and is predicted to target bacterial peptidoglycan specifically. Recombinant endolysin S2 was efficiently expressed in a soluble form in *E. coli* BL21 (DE3) and showed no adverse effects on host cell growth, indicating good biocompatibility. Notably, the introduction of a 6 × His tag at the N-terminus of endolysin S2 not only did not affect its recombinant expression but also significantly improved protein solubility and

subsequent purification yield. The recombinant protein was efficiently purified using nickel-affinity chromatography, yielding a high-purity preparation of endolysin S2. This purified endolysin serves as a crucial foundation for subsequent functional characterisation and application development.

Bacteriophage endolysins are proteins encoded by double-stranded DNA bacteriophages that specifically hydrolyse glycosidic bonds within the bacterial peptidoglycan layer [17]. Their mechanism of action on conserved targets makes the development of bacterial resistance unlikely. Due to significant differences in bacterial extracellular structures across species [18], endolysins can achieve specific recognition, effectively eliminate target pathogens while minimise impact on the host's normal microbiota. In contrast, endolysins target the highly conserved peptidoglycan structure, a mechanism against which bacteria are less likely to develop resistance, thereby offering broader efficacy [19]. In Gram-negative bacteria, the outer membrane (OM) acts as a barrier to endolysin activity. This limitation can be overcome by combining endolysins with OM permeabilisers, such as EDTA, organic acids, or certain antibiotics, to facilitate access to the peptidoglycan layer and achieve effective bactericidal activity.

In this study, the *S. aureus* endolysin S2, identified via viral metagenomics, exhibited increased antibacterial activity against Gram-positive bacteria. Additionally, endolysin S2 exhibited activity against several Gram-negative bacterial strains, including *S.* Enteritidis, *S.* Typhi, *E. coli*, and *Shigella*, following EDTA pretreatment. This requirement for an OM permeabilizer is shared by other well-characterised endolysins, such as *Salmonella* endolysin Gp110 and *Pseudomonas aeruginosa* endolysin LysPA26 [20, 21]. The dependence of endolysin S2 on EDTA concentrations suggests that it may possess exceptional OM penetration efficiency or peptidoglycan hydrolysis activity. This property implies a potentially lower risk of cytotoxicity and improved biocompatibility, which are advantageous for applications in complex environments such as food processing. TEM micrographs revealed that treatment with 100 μg/ml endolysin S2 resulted in the most severe morphological damage to bacterial cells. Endolysin S2 exhibited lytic activity not only against its host bacterium, *S. aureus* ATCC12600, but also against EDTA-pretreated *Shigella sonnei*. Compared with the control, treated cells displayed loss of membrane integrity and cellular disintegration, confirming the bacteriolytic effect of endolysin S2, as shown in TEM images. Currently, there is a relative lack of studies on endolysins for *Shigella*; however, the present study found that endolysin S2 exhibits lytic activity against *Shigella*, including *Shigella sonnei*, *Shigella flexneri*, *Shigella dysenteriae*, and *Plesiomonas shigelloides*. Notably, endolysin S2 exhibited a significant lytic effect on *Shigella sonnei*. These findings not only address a gap in Shigella-specific endolysin research but also identify endolysin S2 as a promising candidate for the development of novel therapeutics against *Shigella* infections.

The lytic activity of endolysin S2 was significantly influenced by environmental pH and temperature. The optimal activity conditions for endolysin S2 were closely matched with the processing and storage environments of many common foodstuffs in China. It exhibited lytic activity across a broad pH range from weakly acidic to weakly alkaline, with an optimum at pH 8.0. This pH profile matches well with various food products, such as traditional Chinese fermented foods (e.g., soya bean paste, pH 7.5–8.0), fresh animal meat (pH 5.6–6.8), and aquatic products (pH 6.5–7.0). The optimal activity of endolysin S2 was observed at 25 °C. Notably, more than 90% of its relative activity was maintained at 37 °C, indicating its suitability for various food processing techniques conducted at ambient temperatures, such as pickling and fermentation. These characteristics make endolysin S2 a promising candidate for the microbial control of traditional fermented foods, the preservation of fresh meat, and the development of preservative additives for neutral-pH foods.

In conclusion, our study demonstrates that endolysin S2 exhibits optimal lytic activity at 25 °C and pH 8.0. Endolysin S2 was effective not only against its parental strains but also against a range of other bacterial species. Specifically, endolysin S2 proved effective against multiple *S. aureus* genotypes and other foodborne pathogens.

Due to limitations of *in vitro* experiments, the safety of the endolysin in humans, its bactericidal activity on food and biofilm surfaces, and the use of a fluorescent probe to investigate the binding site can be further explored in future studies.

CONCLUSION

In this study, we identified and characterised a novel *S. aureus* endolysin, designated S2, from environmental water samples using viral metagenomics. Endolysin S2 exhibited lytic activity not only against *S. aureus* but also against a range of Gram-negative pathogens, including *S.* Enteritidis, *S.* Typhi, *E. coli*, and *Shigella*. The optimal lytic activity of endolysin S2 was observed at 25 °C and at pH 8.0. Given its marked antibacterial properties, future studies should evaluate the efficacy of endolysin S2 in food models and specific application environments to fully assess its potential as a biocontrol agent against foodborne pathogens.

Acknowledgements: This work was supported by the Talents Recruitment Grant of the Yangfan Plan of Guangdong Province (4YF16003G), the Dongguan Science and Technology of Social Development Program (20231800936342) and the Undergraduate Innovation and Entrepreneurship Education Base Project of Guangdong Medical University (JDXM2024029 & JDXM2024075).

REFERENCES

1. Tong SYC, Fowler VG Jr, Skalla L, Holland TL (2025) Management of *Staphylococcus aureus* bacteremia: A review. *JAMA* **334**, 798–808.
2. Tribuddharat C, Pummangura C, Srifuengfung M, Pipobwatthana P, Thuncharoon H, Rodjun V, Chongtrakool P, Srifuengfung S (2022) Prevalence and antimicrobial susceptibility of methicillin-resistant *Staphylococcus aureus* clones: A study at Taksin Hospital, Bangkok, Thailand. *ScienceAsia* **48**, 159–164.
3. Wongthong S, Kamonsutthipaijit N, Kaewhan C, Chanawong A, Tippayawat P, Lulitanond A (2022) Preliminary study on small angle x-ray scattering patterns of intact vancomycin susceptible and non-susceptible *Staphylococcus aureus* cells. *ScienceAsia* **48**, 37–42.
4. Gerstmans H, Criel B, Briers Y (2018) Synthetic biology of modular endolysins. *Biotechnol Adv* **36**, 624–640.
5. Gondil VS, Chhibber S (2021) Bacteriophage and endolysin encapsulation systems: A promising strategy to improve therapeutic outcomes. *Front Pharmacol* **12**, 675440.
6. Rahman MU, Wang W, Sun Q, Shah JA, Li C, Sun Y, Li Y, Zhang B, et al (2021) Endolysin, a promising solution against antimicrobial resistance. *Antibiotics (Basel)* **10**, 1277.
7. Mirski T, Lidia M, Nakonieczna A, Gryko R (2019) Bacteriophages, phage endolysins and antimicrobial peptides: The possibilities for their common use to combat infections and in the design of new drugs. *Ann Agric Environ Med* **26**, 203–209.
8. Vasina DV, Antonova NP, Grigoriev IV, Yakimakha VS, Lendel AM, Nikiforova MA, Pochtovyi AA, Remizov TA, et al (2021) Discovering the potentials of four phage endolysins to combat gram-negative infections. *Front Microbiol* **12**, 748718.
9. Lambrechts S, Willems A, Tahon G (2019) Uncovering the uncultivated majority in antarctic soils: Toward a synergistic approach. *Front Microbiol* **10**, 242.
10. Bateman A, Rawlings ND (2003) The chap domain: A large family of amidases including gsp amidase and peptidoglycan hydrolases. *Trends Biochem Sci* **28**, 234–237.
11. Modi M, Thambiraja M, Cherukat A, Yennamalli RM, Priyadarshini R (2024) Structure predictions and functional insights into amidase_3 domain containing n-acetylmuramyl-l-alanine amidases from deinococcus indicus dr1. *BMC Microbiol* **24**, 101.
12. Sanz-Gaitero M, Keary R, Garcia-Doval C, Coffey A, van Raaij MJ (2014) Crystal structure of the lytic chap(k) domain of the endolysin lysk from *Staphylococcus aureus* bacteriophage k. *Virol J* **11**, 133.
13. Gu J, Feng Y, Feng X, Sun C, Lei L, Ding W, Niu F, Jiao L, et al (2014) Structural and biochemical characterization reveals lysgh15 as an unprecedented "ef-hand-like" calcium-binding phage lysin. *PLoS Pathog* **10**, e1004109.
14. Mek-yong K, Jiangjamjit K, Napaswad C, Homkaew A, Chabang N, Thongpanchang T, Dubbs P, Soodvilai S (2025) *In vitro* antibacterial activity of panduratin a and its derivatives against vancomycin-resistant *Entercoccus faecium* clinical isolates. *ScienceAsia* **51**, ID 2025020.
15. Malachowa N, DeLeo FR (2010) Mobile genetic elements of *Staphylococcus aureus*. *Cell Mol Life Sci* **67**, 3057–3071.
16. Wang S, Li X, Yang W, Huang R (2024) Exploring the secrets of marine microorganisms: Unveiling secondary metabolites through metagenomics. *Microb Biotechnol* **17**, e14533.
17. Grabowski Ł, Łepek K, Stasiłojć M, Kosznik-Kwaśnicka K, Zdrojewska K, Maciąg-Dorszyńska M, Węgrzyn G, Węgrzyn A (2021) Bacteriophage-encoded enzymes destroying bacterial cell membranes and walls, and their potential use as antimicrobial agents. *Microbiol Res* **248**, 126746.
18. Fernandes S, São-José C (2016) More than a hole: The holin lethal function may be required to fully sensitize bacteria to the lytic action of canonical endolysins. *Mol Microbiol* **102**, 92–106.
19. Arakelian AG, Chuev GN, Mamedov TV (2024) Molecular docking of endolysins for studying peptidoglycan binding mechanism. *Molecules* **29**, 5386.
20. Rodríguez-Rubio L, Gerstmans H, Thorpe S, Mesnage S, Lavigne R, Briers Y (2016) Duf3380 domain from a salmonella phage endolysin shows potent n-acetylmuramidase activity. *Appl Environ Microbiol* **82**, 4975–4981.
21. Guo M, Feng C, Ren J, Zhuang X, Zhang Y, Zhu Y, Dong K, He P, et al (2017) A novel antimicrobial endolysin, lyspa26, against *Pseudomonas aeruginosa*. *Front Microbiol* **8**, 293.